Bull. Fac. Fish. Hokkaido Univ.
41(1), 32-42. 1990.

Studies on Acoustic Target Strength of Squid VI. Simulation of squid target strength by prolate spheroidal model

I Nyoman ARNAYA* and Noritatsu SANO*

Abstract

Characteristics and general trends of the target strength of squid with special reference to surume ika (*Todarodes pacificus*) were investigated by using a liquid prolate spheroidal model. Backscattering amplitudes were calculated for the liquid prolate spheroid having typical morphological and physical parameters of actual squid. Those backscattering amplitudes were shown as frequency and size (body length and thickness) dependences, the backscattering patterns, the density and sound speed dependences, and orientation dependence. These results were compared with experimentally measured target strength data and good agreement was found.

The frequency dependence of dorsal aspect target strength of squid is small at $L/\lambda > 2$ (in this geometrical region, target strength is approximately proportional to the squared body length), and has a Rayleigh region at $L/\lambda \ll 1$, but there is no resonant scattering between the two regions. The density and sound speed range observed for squid causes variability of about 5 to 20 dB in the target strength value. The variability of target strength with respect to the orientation is very high due to the very directive backscattering patterns when L/λ and body thickness are not small.

Introduction

A squid as an acoustic target in the sea resembles a spheroid, or something similar to a spheroid such as a finite length of cylinder. Because of its elongated shape, a finite length cylinder is a potential candidate for modelling a squid, and has often been used for bladder fish and other marine organisms. However, a spherical model will fail to predict the broadside scattering of a squid's elongated body.

As was observed in the previous study[1~5], the prominent factors which determine values and characteristics of the squid target strength are: (1) body length and shape, (2) ensonifying frequency, (3) structural components of the body and their physical parameters, especially density and sound speed (acoustic impedance), (4) orientation and behaviour, and (5) swimming movement. Hence, using a proper theoretical model, we need to be able to predict target strength, interpolate or extrapolate measured data, and propose measuring methods.

Squid, which lack a swimbladder (bladderless fish) and have a cylindrical or elongated body shape, need a suitable model not only to describe the characteristics of their target strength but also to enable prediction of the general trends. A prolate spheroid (FURUSAWA's model)[1] and fluid-deformed cylinder of finite length (STANTON's model)[7,8] may meet the requirements as theoretical (acoustic) models.

* *Laboratory of Instrument Engineering for Fishing, Faculty of Fisheries, Hokkaido Univereity*
(北海道大学水産学部漁業測器学講座)

The usefullness of the liquid spheroidal model was mentioned by FURUSAWA[6], but due to the limited precision of the computer in the computation, it is difficult to predict general trends of target strength for L/λ above 4. If we apply this model for squid, the values of measured-target-strengths are outside of the computational range, so that direct comparison can not be made. This will be solved by extending the L/λ range of his model and comparing the results with the experimental data. On the other hand, the fluid cylinder model is promising, but this could not give good predictions on such directive scatterers as squid and cannot reasonably explain the results obtained by recent precise observations.

Consequently, here we adopt a liquid prolate spheroid as the scattering model of squid, calculate the scattering characteristics, especially backscattering amplitudes, and simulate the general trends of squid target strength.

Materials and Methods

1. *Modelling of squid*

Squid, which are the only truly nektonik invertebrates, live and compete in the open ocean with fish and mammals using a propulsive system totally unlike that of their predators and competitors. The fundamental body divisions of squid have apparently nothing remotely in common with the arrangement in fish. There is no morphological fish equivalent of a mantle sac, arms and a head in the middle of the body. Jet propulsion[5], the mode of locomotion typical of common squid has been developed as an accessory means of moving in only a few fish. Yet a squid, when separated from its fellows in an aquarium tank, will shoal instead with sardines; apparently it finds them "like" itself. They too are streamlined, the body maintains its outline and does not bend in the vertical plane, they move at similar speeds along their long axis, and above all, they swim in shoals.

Like fish the squid body is designed for suspension, the stiff supporting members located dorsally and the viscera hanging below. Cross sections of a common squid and a perciform fish illustrate this well. Squid have rounded cross-sections and stream-lining forms. The shape of the body changes as the squid grows[9] from a short and stubby larva with a diameter of about one-third of the body length, to a slender torpedo-shape when an adult (Fig. 1). As shown in this figure, the adult mean diameter of fast swimming squid (B) is about one-eighth their body-length (without including the tentacles): a value close to that typical of scombrid fish (A). In both fish and squid the level at which the largest cross section is to be found passes progressively backwards with increasing body size and swimming speed.

Physical parameters and dimensions of squid were examined using our measurements and some references[10,11] especially of surume ika (*Todarodes pacificus*). The upper part of Table 1 shows the approximate ranges and average values of the critical dimensions and physical properties of squid. Parameters for the model are derived from actual squid parameters, and are shown in the lower part of Table 1. The body height and breadth/width are shown in the unit of standard body length L, the length from the root of the tail (caudal fin) to the tip of longest arms. When the density of the seawater (ρ_0) is 1.025 g/cm^3, the density ratio for the average squid density is 1.003. Similarly, when the sound speed in the seawater (c_0) is 1,500 m/s, the ratio for the average squid sound speed is 1.007.

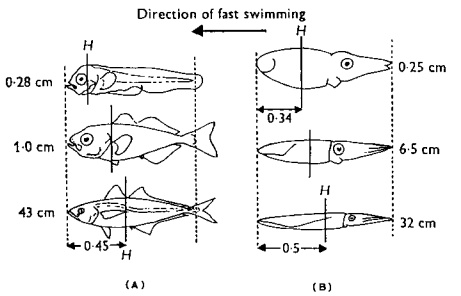

Fig. 1. Hydrodynamic shape of squid and scombrid fish. Changes in the position of greatest body height(H) during ontogeny, (A) in a fish, the horse mackerel (*Trachurus* spp), (B) in the squid (*Loligo vulgaris*). In both the squid and the fish, H shifts backwards during ontogeny to a region typical of "good swimmers". This region is between 0.4 and 0.56 along the length of the body.

Table 1. Morphological and physical parameters of squid and model

		Body Height ($\times L$)	Body Width ($\times L$)	Density (g/cm^3)	Sound speed (m/s)
Squid	Min.	0.14	0.14	1.010	1492
	Ave.	0.16	0.16	1.028	1510
	Max.	0.18	0.18	1.045	1528
			b/a	ρ_1/ρ_0	c_1/c_0
Model	Min.		0.10	0.985	0.995
	Ave.		0.15	1.003	1.007
	Max.		0.20	1.20	1.019

*) L is standard length, a is major radius, b is minor radius, ρ_0 is density of seawater ($=1.025$ g/cm^3), ρ_1 is density of squid body, c_0 is sound speed in seawater (1,500 m/s), and c_1 is sound speed in squid body.

Fig. 2 shows the geometry of the squid and models. The squid body, in general, inclines in a way in which the posterior part rises as shown in Fig. 2(A). Since this affects sound scattering, so that this inclination or tilt angle, θ_t, as measured from a horizontal line, is also shown. Fig. 2(B) shows the shape of the model used. The aspect ratio of the body is noted by (b/a), where a is the major radius, and b is the minor radius. More detailed explanations of these parameters will be given in the following section.

2. *Computational method*

Scattering amplitude of a liquid spheroid[6,12,13] is determined by solving the scalar wave equation in spheroidal coordinates and applying the respective boundary conditions. Spheroidal wave functions[14] appear in the results and they are not easy to calculate. Therefore, previous scattering calculations have been often restricted to special cases.

The prolate spheroidal coordinate system is generated by rotating the two-dimensional elliptic coordinates system about the major axis z. This prolate spheroidal coordinates (ξ, η, ϕ) shown in Fig. 3 are related to the rectangular Cartesian coordinates (x, y, z) by the transformation[14,15],

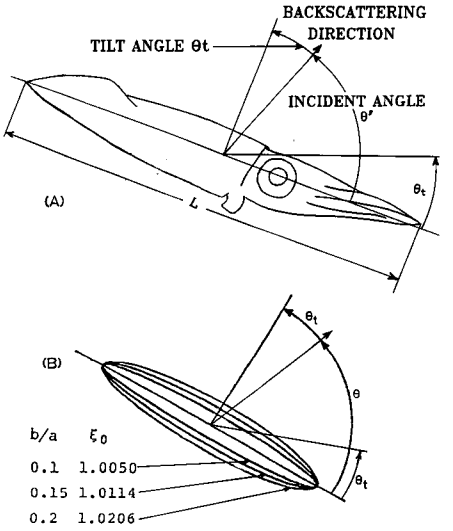

Fig. 2. Geometry of squid (A) and model (B).

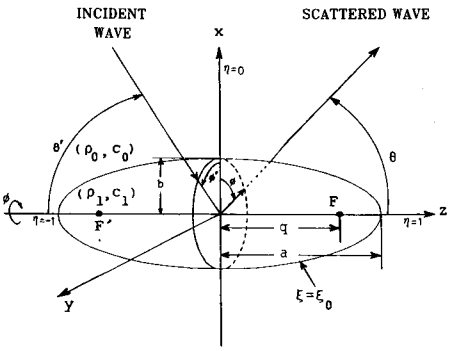

Fig. 3. Prolate spheroidal coordinates and relevant parameters.

$$
\begin{aligned}
x &= (d/2)[(\xi^2-1)(1-\eta^2)]^{1/2}\cos\phi,\\
y &= (d/2)[(\xi^2-1)(1-\eta^2)]^{1/2}\sin\phi,\\
z &= (d/2)[\xi\eta].
\end{aligned}
\tag{1}
$$

The interfocal distance of the generating ellipse is denoted by d. The coordinates ξ represent a family of ellipsoids of revolution with common focal points. This radial coordinate, ξ, may range from one for an infinitely thin needle to ∞ for a sphere of infinite radius. The spheroid of constant ξ has a major length $L=\xi d=2a$ (a is major radius) and a minor radius $b=(d/2)(\xi^2-1)^{1/2}$. The fineness ratio is a/b and the eccentricity of the spheroid is $1/\xi$. The hyperbolic (or angle) coordinate, η, is associated with hyperbolic surfaces that are orthogonal to the confocal ellipsoids. $\eta=\pm 1$ refers to the $\pm z$ axis, respectively, and $\eta=0$ defines the $x-y$ plane that passes through the equator (midsection) of the spheroid. The angle between the z axis and asymptotic cone associated with the hyperbola $\eta=$constant is simply $\phi=\cos^{-1}\eta$. When $\xi\gg 1$, this angle is analogous to the spherical aspect angle θ. The rotational coordinate ϕ ranges from 0 (x axis) to 2π and is identical to the spherical coordinate ϕ for all ranges of ξ and η.

A spheroid surface is given by $\xi=\xi_0=$constant, where ξ_0 is radial spheroidal coordinate at the buondary of the prolate spheroid. Denoting the major radius a, the minor radius b and the semi-focal length q as described above, we have the following relations:

$$
\begin{aligned}
a &= \xi_0 q\\
\xi_0 &= [1-(b/a)^2]^{1/2}
\end{aligned}
\tag{2}
$$

Density is expressed by ρ, sound speed by c and wavenumber by k, each followed by a subscript o for the surrounding medium or 1 for the spheroidal body.

The computations were made by a HP-BASIC program on a desk-top computer

(HP-9816), similar as described in FURUSAWA's model.[6]

The target strength (TS) is related to the farfield backscattering amplitude f_∞ by :

$$TS = 20 \log F = 20 \log |f_\infty(\theta, 0 | \pi - \theta, \pi)| \tag{3}$$

wher F is defined as the absolute value of the farfield backscattering amplitude. Here, the term target strength is used both for the decible value, TS, and the intensity ratio, i.e., F^2. Its clear that the backscattering amplitude is a function of angles (θ, ϕ, θ', ϕ'), shape (ξ_0 or b/a), wavenumber (k_0), and the density ratio (ρ_1/ρ_0). If f_∞ of Eq. (3) is normalized by $2a$, a variable conveniently disappears since $k_0 a = h_0/\xi_0$, where h_0 is reduces frequency ; therefore, $F/2a$ is calculated.

The frequency dependence of scattering is often exhibited as a function of $k_0 a$. In fisheries acoustics, however, the ratio of body length to wavelength, L/λ, has been commonly used. The relations for the two schemes are :

$$L/\lambda = (1/\pi) k_0 a \tag{4}$$

Recently, experimental values of target strength have been normalized by the square of body length L in centimeters and expressed as

$$TS = A + 20 \log L \tag{5}$$

This A, which is equal to the TS value of one centimeter length of the squid, corresponds to the theoretical value $F/2a$ and the relation is

$$A = 20 \log (F/2a) - 40 \tag{6}$$

The average dorsal aspect target strengths is commonly used to estimate the body length and abundance of squid. For obtaining the average dorsal aspect target strength with respect to orientation, here we only need to consider the tilt angle of the body. The tilt angle θ_t is defined as shown in Fig. 2, and the sign is negative when the squid looks downward and positive when upward. The averaging process for our theoretical case is[6] :

$$\langle (F/2a)^2 \rangle = \int [F(\theta)/2a]^2 g(\theta_t) d\theta_t \Big/ \int g(\theta_t) d\theta \tag{7}$$

where $g(\theta_t)$ is the probability desity function of the tilt angle of squid[2,16]. As can be seen from Fig. 2, the backscattering direction is $\theta = \pi/2 - \theta_t$. An orientation distribution ($g(\theta_t)$) or the corresponding averaging mode by Equation (7) is simply denoted by an angle pair such as ($\bar{\theta}_t$, $s_{\theta t}$), where $\bar{\theta}$ is the mean tilt angle, and $s_{\theta t}$ is the standard deviation of the tilt angle. This notation is used also for a constant orientation as ($\bar{\theta}_t$, 0).

Results and Discussion

1. *Backscattering characteristics of a liquid prolate spheroid*

In this section, we illustrate the results of numerical calculations mainly of the backscattering characteristics of the present liquid prolate spheroidal model because of our concern with target strength.

Figure 4 shows the backscattering characteristics as functions of $k_0 a$ for liquid prolate spheroid with typical parameters given in Table 1. The backscattering direction for Fig. 4(A) is 90° (broadside incidence) and for Fig. 4 (B) is 0° (end-on

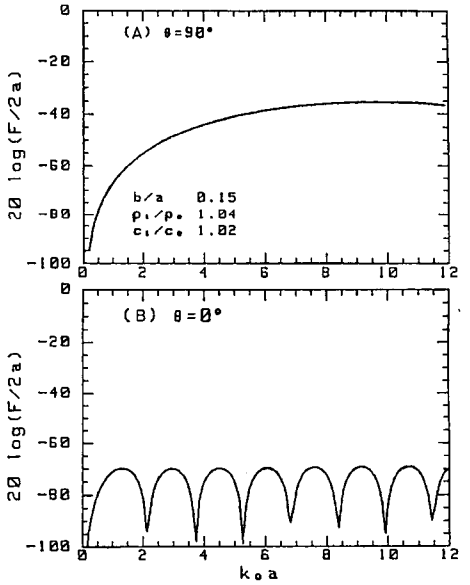

Fig. 4. Backscattering amplitudes as functions of k_0a for liquid prolate spheroid with typical parameters of squid. Incident angle is 90° for (A) and 0° for (B).

incidence). As shown in the Fig. 4(A), for the 90° backscattering direction the liquid prolate spheroid exhibit Rayleigh scattering at small k_0a and becomes almost flat at larger k_0a. For the 0° backscattering direction, the amplitude of the liquid prolate spheroid fluctuates with increasing k_0a, rather similar to those of liquid spheres[17], but differs drastically from those of broadside incidence. Therefore, the spherical model will fail to predict the broadside scattering of an elongated body or directional scatterers such as squid. Furthermore, the Rayleigh model is applicable at $L/\lambda \ll 1$, but cannot applied at larger L/λ.

Backscattering patterns are shown in Fig. 5. From the left to the right k_0a is increased by a factor of 3, and from the top to the bottom thickness b/a is varied as 0.10, 0.15 and 0.20 (see Table 1 and Fig. 2(B)). As k_0a increases the number of lobes increases, and the pattern of the scattering components becomes unstable. However, it is clear that the liquid prolate spheroid's backscattering pattern has a main (prominent) lobe and side lobes. When the thickness (b/a) is varied, the broadside backscattering amplitude changes significantly especially for small k_0a values. Thus, the backscattering patterns are very directive and dependent on both the k_0a and the thickness or minor radius b of the body.

The effect of the density and sound speed contrasts on the backscattering of a liquid prolate spheroidal body is shown in Fig. 6. When the density ratio is small, the scattering strength varies greatly with the sound speed ratio and vice versa. Considering the range of the parameters values shown in Table 1 and Fig. 6, we suffer a variation of 5-20 dB in the target strength of squid. Hence, measurements of the target strength of squid must be carried out in seawater, because of the great target strength variability with respect to the density and sound speed contrasts between the body and surrounding medium.

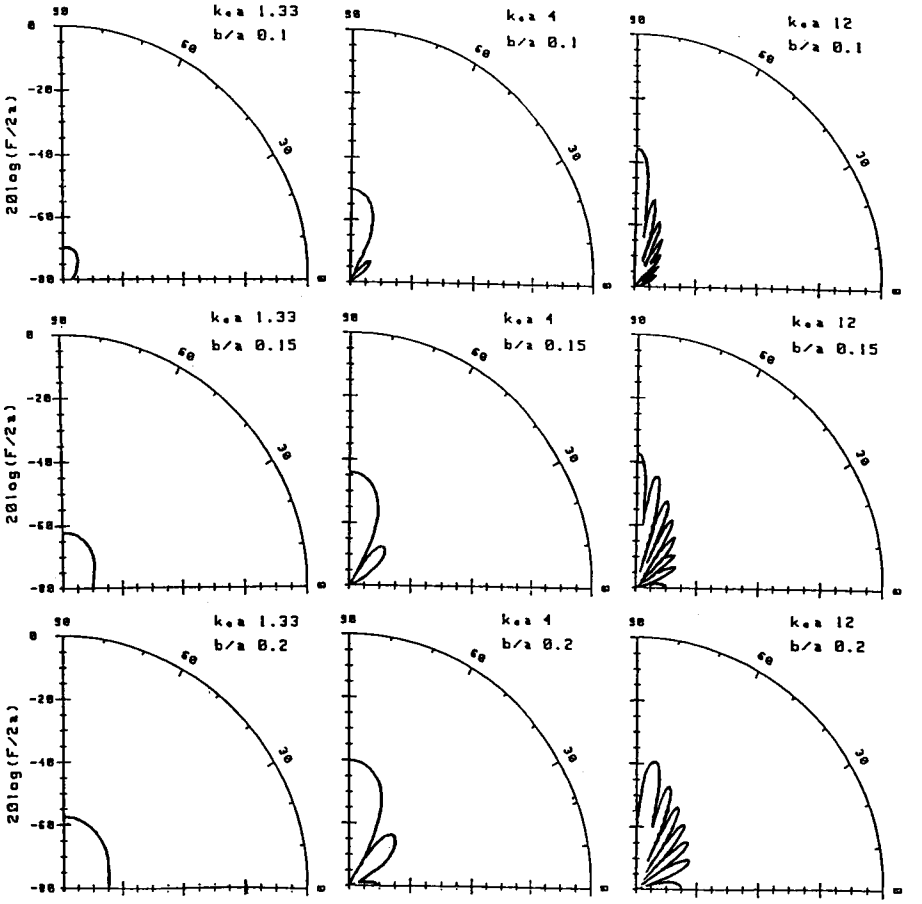

Fig. 5. Backscattering patterns of liquid prolate spheroid. From left to right k_0a is increased by a factor of 3, and from top to bottom, aspect ratio or thickness b/a is varied as 0.1, 0.15, 0.2. Density and sound speed ratios are 1.04 and 1.02, respectively.

2. *Effect of orientation on target strength*

Fig. 7 shows the normalized target strengths or A-values for the liquid prolate spheroid or bladderless model of $b/a=0.15$ with respect to several orientations or averaging modes as functions of L/λ.

In the Figure, $(-6, 0)$ means the constant tilt angle of $-6°$ and a standard deviation of 0°. The orientation (0, 0) corresponds to the horizontal posture. The other three curves of Fig. 7 show the results averaged with respect to orientation or averaging mode by Eq. (7).

As shown in the Figure, the horizontal orientation (0, 0) gives the maximum dorsal-aspect target strength. When a squid looks downward by 6°, as seen from the curve denoted by $(-6, 0)$, a strong negative trend appears at large L/λ. At small L/λ the A-values are very similar among orientation distributions because of

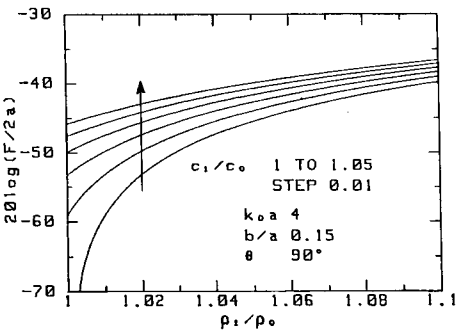

Fig. 6. Effect of density and sound speed contrasts on backscattering amplitude for liquid prolate spheroid.

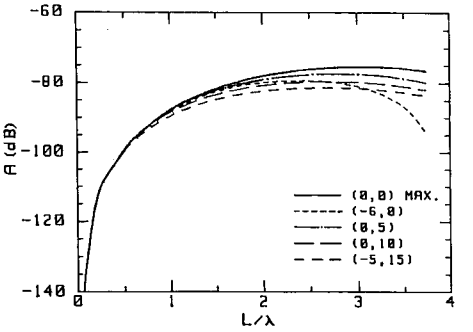

Fig. 7. Effect of orientation or averaging on near-broadside-aspect normalized-target-strength of liquid prolate spheroid of aspect ratio or thickness $b/a=0.15$ as functions of L/λ.

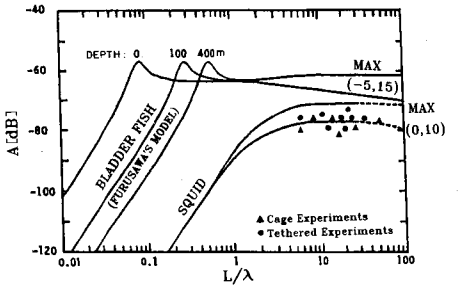

Fig. 8. Comparisons of normalized-target-strengths measured for surume ika (*Todarodes pacificus*) and those derived theoretically for liquid prolate spheroidal model and comparisons of general trends of normalized-target-strength for bladder fish and squid (bladderless fish).

omnidirectional scattering patterns, but there are large variations in the target strength value when the orientation changes where L/λ is not small. In general, at larger $L/\lambda(>2)$ the dependence of the normalized target strength A on L/λ is small. This means that the frequency dependence of the dorsal aspect target strength is small and the value is nearly proportional to the squared body length. Therefore, it is reasonable to express the target strength as Eq. (5). Thus, we propose to express the target strength of squid by normalizing it by squared body length, attaching information on frequency and orientation or averaging mode.

3. *Comparison with experiments*

The range of L/λ (up to about 4) as seen in Fig. 7 covers only some of our data observed in experiments. The geometrical expression enables us to inspect approximate features beyond the maximum L/λ that is calculable by the exact expressions. However, to understand more complicated characteristics, such as scattering patterns, at first we must extent the calculable range as much as possible. Then, because the upper limit of L/λ is enough in the geometrical region at least for broadside scattering, we may extrapolate the results and inspect the trends beyond the limit.

In Fig. 8, we compare our cage experiments data[3,4] and tethered experiments

data (unpublished data) observed on surume ika (*Todarodes pacificus*), with the corresponding theoretical results (when the orientation distribution is (0, 10)). Here, only average dorsal aspect target strength data are compared because of unsufficient data concerning maximum dorsal aspect target strength. The dotted line beyond the maximum limit of L/λ is the geometrical approximation obtained by the extrapolation. As shown in the Figure, the theoretical average curve agrees well with all data, but is lower than the theoretical maximum curve.

When the present theoretical results were compared with the well known FURUSAWA's model for bladder fish of different swimming depth, it is clear that bladder fish give higher target strength values by more than 10 dB than squid (bladderless fish) in the geometrical region. But in the Rayleigh region, the target strength values of squid are suddenly very small compared to bladder fish. Furthermore, different from bladder fish, for squid there is no resonant scattering apparent between the Rayleigh region and the geometrical region. The fact that bladderless fish, have smaller target strength values than those of bladder fish, especially in the geometrical region, is supported by FOOTE[18], McCARTNEY and STUBBS[19], EDWARDS and ARMSTRONG[20], MacLENNAN *et al.*[21,22], and ROSE and LEGGETT[23] experiments on Atlantic mackerel, a swimbladderless fish.

Conclusion

A squid as an acoustic target in the sea resembles a spheroid, or something similar to a spheroid such as a finite length cylinder. From the present simulation, a liquid prolate spheroid is shown to be a good model to describe the scattering characteristics of squid and to predict general trends of its dorsal aspect target strength.

The frequency dependence of the dorsal aspect target strength of squid is small at $L/\lambda > 2$ (in this geometrical region, target strength is approximately proportional to the squared body length), and has a Rayleigh region at $L/\lambda \ll 1$. However, there is no resonant scattering apparent between the Rayleigh region and the geometrical region. In addition, the thickness or shape of the body has a significant effect on the dorsal aspect target strength. When insonified end-on, the frequency characteristics differ drastically from those of broadside incidence (dorsal aspect). These end-on scattering characteristics have similar features to those of a spherical model, so it follows that the spherical model will fail to predict the broadside scattering of an elongated body, such as squid.

The density and sound speed range observed for squid causes variability of about 5 to 20 dB in the target strength value. Since the target strength value is in itself very small (compared with bladder fish), other morphological and anatomical components such as tentacles, dorsal pen, viscera, gonad, gill and other internal organs will affect the scattering strength. It is also suggested that another cause of variability in the target strength is that the density and sound speed of a squid's body varies with its growth or ontogeny and temperature. Hence, measurements of the target strength of squid must be carefully carried out. They must be measured in seawater, the composition of the body and physical parameters must be specified as functions of their growth and surrounding, and the orientation must be precisely observed.

The variability of squid target strength with respect to the orientation is very high, due to the very directive backscattering patterns when L/λ is not small. At small L/λ the target strength values are very similar in orientation distribution because of omnidirectional scattering patterns.

Much work remains to be done. As with every scattering model, the limitations of this model, especially the range of L/λ in our computation, need to be explored. The accuracy of the present model in application needs to be investigated through field (*in situ*) experimentation and more controlled experimentation so that reliable predictions of target strength and inversion of its data to predict body length of squid may be performed.

Acknowledgements

The authors are grateful to Dr. M. FURUSAWA of National Research Institute of Fisheries Engineering for his aid in the computer programming of this difficult prolate spheroidal model. The authors also express their appreciation to Dr. K. IIDA and Mr. T. MUKAI, Lecturer and Instructor, respectively, of the Laboratory of Instrument Engineering for Fishing, Faculty of Fisheries, Hokkaido University, for their useful suggestions and assistance.

References

1) Arnaya, I., Sano, N., and Iida, K. (1988). Studies on acoustic target strength of squid. I. Intensity and energy target strengths. *Bull. Fac. Fish. Hokkaido Univ.*, **39**, 187-200.
2) Arnaya, I., Sano, N., and Iida, K. (1989). Studies on acoustic target strength of squid. II. Effect of behaviour on averaged dorsal aspect target strength. *Bull. Fac. Fish. Hokkaido Univ.*, **40**, 83-99.
3) Arnaya, I., Sano, N., and Iida, K. (1989). Studies on acoustic target strength of squid. III. Measurement of the mean target strength of small live squid. *Bull. Fac. Fish. Hokkaido Univ.*, **40**, 100-115.
4) Arnaya, I., Sano, N., and Iida, K. (1989). Studies on acoustic target strength of squid. IV. Measurement of the mean target strength of relatively large-sized live squid. *Bull. Fac. Fish. Hokkaido Univ.*, **40**, 169-181.
5) Arnaya, I. and Sano, N. (1990). Studies on acoustic target strength of squid. V. Effect of swimming on target strength of squid. *Bull. Fac. Fish. Hokkaido Univ.*, **41**, 18-31.
6) Furusawa, M. (1988). Prolate spheroidal models for predicting general trends of fish target strength. *J. Acoust. Soc. Jpn. (E)*, **9**, 13-24.
7) Stanton, T.K. (1988). Sound scattering by cylinders of finite length. I. Fluid cylinders. *J. Acoust. Soc. Am.*, **83**, 55-63.
8) Stanton, T.K. (1989). Sound scattering by cylinders of finite length. III. Deformed cylinders. *J. Acoust. Soc. Am.*, **86**, 691-705.
9) Zuev, G.V. (1964). The body shape of cephalopods. *Trudy Sevast. Biol. Stants.*, **17**, 379-387. (in Russian).
10) Hashimoto, T., Nishimura, M., Maniwa, Y. and Motegi, K. (1952). Study on school finder. *Tech. Rep. Fish. Boat*, **3**, 177-234. (in Japanese).
11) Hashimoto, T., Maniwa, Y. and Motegi, K. (1953). Study on fish finder. V. Ultrasonic reflection loss of fish body. *Tech. Rep. Fish. Boat*, **4**, 143-153. (in Japanese).
12) Yeh, C. (1964). The diffraction of sound waves by penetrable disks. *Ann. Phys.*, **7**, 53-61.
13) Yeh, C. (1967). Scattering of acoustic waves by a penetrable prolate spheroid. I. Liquid prolate spheroid. *J. Acoust. Soc. Am.*, **42**, 518-521.
14) Flammer, C. (1957). Spheroidal Wave Functions. *Univ. Press*, Stanford.

15) Lauchle, G.C. (1975). Short-wavelength acoustic diffraction by prolate spheroids. *J. Acoust. Soc. Am.*, **58**, 568-575.
16) Foote, K.G. (1980). Averaging of fish target strength functions. *J. Acoust. Soc. Am.*, **67**, 504-515.
17) Anderson, V.C. (1950). Sound scattering from fluid sphere. *J. Acoust. Soc. Am.*, **22**, 426-431.
18) Foote, K.G. (1980). Importance of the swimbladder in acoustic scattering by fish : A comparison of gadoid and mackerel target strength. *J. Acoust. Soc. Am.*, **67**, 2084-2089.
19) McCartney, B.S. and Stubbs, A.R. (1971). Measurements of the acoustic target strength of fish in dorsal aspect, including swimbladder resonance. *J. Sound Vib.*, **15**, 397-420.
20) Edwards, J.I. and Armstrong, F. (1983). Measurement of target strength of live herring and mackerel. *FAO Fish. Rep.*, **300**, 69-77.
21) MacLennan, D.N., Magurran, A.E., Pitcher, T.J. and Hollingworth, C.E. (1987). Behavioural determinants of fish target strength. *Int. Symp. Fish. Acoust.*, June 22-26, 1987 Seattle, WA, USA. 22 pp.
22) MacLennan, D.N., Hollingworth, C.E. and Armstrong, F. (1989). Target strength and tilt angle distribution of caged fish. *Proc. Int. Acoust.*, **11(3)**, 11-20.
23) Rose, G.A. and Leggett, W.C. (1988). Hydroacoustic signal classification of fish schools by species. *Can. J. Fish. Aquat. Sci.*, **45**, 597-604.